Diffusion on deterministic and quasirandom models of diffusion-limited aggregates I. Isotropic diffusion

Hernan L. Martinez, Juan M. R. Parrondo,* and Katja Lindenberg
Department of Chemistry and Institute for Nonlinear Science, University of California, San Diego, La Jolla, California 92093-0340
(Received 17 February 1993)

We discuss the diffusion of a particle on deterministic and quasirandom fractal structures designed to mimic the properties of diffusion-limited aggregates. In this paper we deal with unbiased transport, while the following paper deals with transport in the presence of an external field. Our method is based on a renormalization procedure that allows us to calculate the scaling properties relating distance and time. We calculate the random-walk dimension d_w for a variety of structures and show how this dimension depends on the branching properties of the model. We find that random walks on these structures become slower as the branching intricacies of the model increase.

PACS number(s): 05.40.+j, 02.50.−r

I. INTRODUCTION

Physical systems with disorder do not possess translational symmetry. Instead, many disordered systems show scale invariance, at least within some finite range of scales. Although not all disordered systems are necessarily fractal, the fact that fractal structures are characterized by scale invariance suggests that the study of physical phenomena in the latter may shed some light on the understanding of such phenomena in the former. Our ultimate purpose is to gain a greater understanding of transport processes in disordered media, a goal that we hope to approach by considering such processes on fractal structures.

Diffusion-limited aggregation (DLA), a growth process first introduced by Witten and Sanders [1], yields fractal structures that have been of enormous interest because they appear to mimic a large number of naturally occurring systems. In this process, monomers start from infinity and diffuse by performing a random walk until they stick to the growing cluster. Physical phenomena that exhibit properties similar to DLA include electrodeposition [2], dielectric breakdown [3], crystallization [4,5], and viscous fingering [6]. As a result, DLA and random walks on diffusion-limited aggregates have been the subject of extensive numerical studies in the past decade [7].

Scale invariance in random fractals such as DLA's and in disordered physical systems holds only in an approximate statistical sense: such fractals look *approximately* equal (but not necessarily identical) on all scales. Deterministic and quasirandom fractals, on the other hand, show strict scale invariances which facilitate the use of analytic techniques for the study of transport on such systems [7]. In particular, it is possible to construct a renormalization procedure for continuous-time random walks on deterministic and quasirandom fractal structures. The renormalization is established between the probability densities of waiting times on an original (fractal) lattice and on the lattice that remains after a particular set of sites has been removed ("decimated" [8] lattice). This procedure was first developed by Machta [9] for a one-dimensional lattice and later by Van den Broeck [10] for a number of finitely ramified fractals. Van den Broeck derived the appropriate renormalization equations and was able to solve a number of them analytically to find asymptotic first-passage-time distributions on these fractals. We have generalized his procedure to account for the presence of a field. This generalization introduces spatial anisotropies that ultimately lead to renormalization schemes involving matrices of hopping probabilities. Specifically, we considered the first-passage-time distribution on a Sierpinski gasket in the presence of an external field [11]. For this system, we found the scaling connections between time, distance and field intensity.

Herein we extend the previous analysis to unbiased walks on two model systems. The first is a deterministic fractal growth model first introduced by Mandelbrot and Vicsek (MV) as a DLA analog [12]. The second is a quasirandom model that introduces space stochasticity and in some important ways attempts to mimic the shapes of random fractals and in particular of some DLA type of structures. Transport on these structures in the presence of an external field is studied in the following paper [13].

In Sec. II we describe both the MV deterministic model of DLA and the quasirandom model that we propose. In Sec. III we discuss in detail the case of isotropic diffusion on the MV model. Isotropic diffusion on the quasirandom model is discussed in Sec. IV. We summarize our results in Sec. V.

II. DETERMINISTIC AND QUASIRANDOM DLA MODELS

A. MV model

The MV model as originally described in 1989 [12] consists of a generator and a simple branching structure made of three units of the same length which replaces

each unit obtained at a previous step. This replacement follows two construction rules: (1) none of the branches may point in a direction below the horizontal, and (2) no branches are allowed to overlap. To satisfy these rules, the branching structure at each step must in fact be either the generator or its mirror image.

We generalize the original MV model to d dimensions, where d is the embedding Euclidean dimension. The structure involves a generator made of $d+1$ units which replaces each unit obtained at a previous step. A MV model in two dimensions and one in three dimensions, both at their third stage of construction, have been drawn in Figs. 1(a) and 1(b).

B. Quasirandom models

We propose a quasirandom model and a generalized quasirandom model as follows.

The first [Fig. 1(c)] is the quasirandom fractal, for which there are two generators, one consisting of a branching structure made of $d+1$ units and another one consisting of two collinear units. Each unit is replaced by the former with probability v and by the latter with probability $(1-v)$. The second case is the generalized quasirandom fractal for which there are d generators consisting of branching structures ranging from 2 to $d+1$ units and associated probabilities P_k, $k = 1,\ldots,d$. A unit is then replaced by a k-unit generator with probability P_{k-1} where the normalization condition $\sum_{k=1}^{d} P_k = 1$ must hold. For $d = 2$ these two models are of course identical.

The replacement of each unit by a given generator follows in all cases the construction rules of the MV model. The angle between two branches of the generator is fixed at the beginning of the construction and remains constant during the entire process. Further, each unit in the generator is of identical length and scaled down by a factor of 2 from the length of the unit obtained at the previous step. We deal with isotropic diffusion on these model structures. In the following paper [13] we also analyze anisotropic diffusion on the MV and quasirandom fractals in two dimensions. It is important to note that all the models described above are special cases of the generalized quasirandom fractal. We have separated them only for the sake of clarity in the discussion to follow.

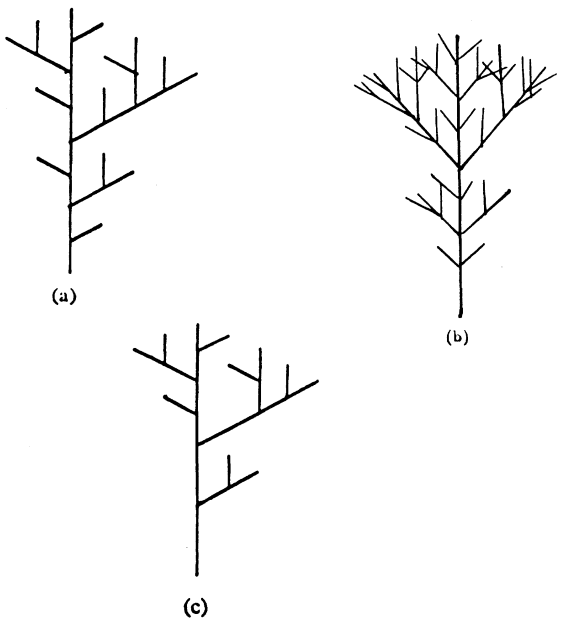

FIG. 1. (a) MV model in two dimensions; (b) generalized MV model in three dimensions; (c) a quasirandom fractal in two dimensions. All are shown at their third stage of construction.

III. RANDOM WALKS ON THE MV MODEL

A. Fractal dimension

In order to describe the properties of a random walk (or diffusion) on a fractal, it is first necessary to establish its fractal dimension d_f. This is done in the usual way by determining the scaling of the mass when a unit is replaced by its generators. In the case of the MV model the mass of unit j is given in terms of the masses of the generators that replace it by

$$m_j(L) = \sum_{i=1}^{d+1} m_i(L/2). \tag{3.1}$$

Since for any unit j the masses of the generators are all equal and independent of j, that is, $m_i = m$, the sum can be done trivially and we can dispense with subscripts to obtain $m(L) = (d+1)m(L/2)$. The scaling of the length by a factor of 2 thus yields a scaling of the mass by a factor of $(d+1)$. Therefore the fractal dimension for the MV fractal in any embedding Euclidean dimension d is

$$d_f = \frac{\ln(d+1)}{\ln 2}. \tag{3.2}$$

B. Renormalization equation and mean waiting time

The continuous-time random-walk formalism [14] based on waiting-time probability densities is sufficiently general to deal with a wide class of random walks. A particle starting at the origin at $t = 0$ performs a nearest-neighbor random walk on a discrete lattice. The waiting time or first-passage time between nearest-neighbor hops is a random variable governed by the hopping-time distribution $\psi_0(t)$. Suppose that the nearest neighbors are removed from explicit consideration, that is, we now focus on the waiting time for hopping between next-nearest neighbors. This time is again a random variable, but the new hopping-time distribution $\psi_1(t)$ will be different from $\psi_0(t)$. The relation between the new distribution and the previous one is the renormalization equation that we are interested in formulating [9,10] to describe transport on the system.

The zero subscript that we have associated with the waiting-time distribution is to be read as "original structure," i.e., the structure with N generations of branches. Let us now implement the following decimation procedure: (1) consider an Nth generation site (the origin of our walk, called a "vertex"), its nearest set of branches, and its next-nearest neighbors; (2) remove from explicit consideration the nearest neighbors that connect the chosen vertex to its next-nearest neighbors. Note that this also removes from explicit consideration the branches that emerge from the nearest neighbors; (3) calculate the first-passage-time distribution from the chosen vertex to any of its next-nearest neighbors (which have now become its nearest neighbors). This last calculation must include all the possible paths connecting the chosen vertex and its next-nearest neighbors through the nearest neighbors that have been removed from explicit consideration. The new results are labeled by the subscript 1. These results allow us to calculate the first-passage-time properties to next-nearest neighbors. Suppose we now repeat this decimation procedure at the next generation. A calculation involving all possible paths on the $(N-1)$st generation structure now yields the hopping probability densities appropriate to the $(N-2)$nd generation structure. These distributions contain the first-passage-time properties for distances of "length" 4 on the original lattice, i.e., each decimation doubles the relevant distances. An N-fold repetition of the procedure then yields information on first-passage times from one extreme of the original structure to the other. Note that in this procedure we fix the total size of the structure; to consider an increasing number of steps in order to calculate asymptotic properties of the walk we increase the number of branch generations N.

Let us first implement the decimation procedure on the MV model to find the renormalization equation. First, we identify two types of vertices in the MV model, the "dead-end" vertex which has one nearest neighbor and the "normal" vertex which has three nearest neighbors. In order to illustrate the calculation we focus first on the dead-end type of vertex. Steps 1 and 2 of the decimation procedure can now easily be visualized from Fig. 2. We have centered our attention on a particular vertex (0) and have marked its only nearest neighbor (1) and associated emerging branch (which ends at site 1′), both of which we want to remove from consideration. In order to calculate the probability density of the decimated lattice, we have to sum over all the possible paths to reach the next-nearest neighbor (a) in time t. This involves a convolution of factors of the undecimated densities [10,11]. It is important to note that next-nearest neighbors can not be reached in an uneven number of steps, that is, the sum of all possibles paths only includes paths that involve an even number of steps.

Following this procedure, one obtains for $\psi_1(t)$ the convolution

$$\psi_1(t) = \sum_{j=1}^{\infty} \frac{N_{2j}}{3^j} \int_0^t dt_{2j-1} \cdots \int_0^{t_2} dt_1 \psi_0(t - t_{2j-1}) \cdots \psi_0(t_2 - t_1)\psi_0(t_1), \tag{3.3}$$

where the walker takes an even number of steps $2j$ with $j = 1, 2, 3, \ldots$ and $N_{2j} = 2^{j-1}$ is the number of different walks of length $2j$ that can bring a walker to the next-nearest neighbor, just as in a one-dimensional walk [10]. The factor $1/3$ associated with every pair of steps reflects the fact that a walker can leave a dead-end vertex in only one way (from 0 to 1), but at the next step the walker has three choices to make ($1 \to 1'$, $1 \to 0$, $1 \to a$), each with probability $1/3$. Two of these possible choices ($1 \to 1'$ and $1 \to 0$) take the walker to a dead-end and the process starts again, and the third ($1 \to a$) takes it to the next-nearest neighbor that ends the walk. The Laplace transform of Eq. (3.3) is

$$\tilde{\psi}_1(s) = \sum_{j=1}^{\infty} \frac{N_{2j}}{3^j} \tilde{\psi}_0^{2j}(s) = \frac{\tilde{\psi}_0^2(s)}{3 - 2\tilde{\psi}_0^2(s)}. \tag{3.4}$$

The decimation procedure at each generation of the process yields the same relation between the waiting-time distributions of two succeeding generations, so that the result Eq. (3.4) can immediately be generalized to

$$\tilde{\psi}_n(s) = \frac{\tilde{\psi}_{n-1}^2(s)}{3 - 2\tilde{\psi}_{n-1}^2(s)}. \tag{3.5}$$

One can perform the same analysis for the dead-end vertex in the higher-dimensional MV model. In this case, the Laplace transform of the hopping probability per pair of steps is $\frac{1}{d+1}\tilde{\psi}_0(s)\tilde{\psi}_0(s)$ and the number of different paths involving an even number of steps is $N_{2j} = d^{j-1}$. Instead of Eq. (3.5) one then obtains the renormalization equation

$$\tilde{\psi}_n(s) = \frac{\tilde{\psi}_{n-1}^2(s)}{(d+1) - d\tilde{\psi}_{n-1}^2(s)}. \tag{3.6}$$

Consider now a walk that begins at a normal vertex, again indicated as vertex 0 in Fig. 2(b). The following relation can immediately be constructed for the waiting time distribution to nearest neighbors (1 or 2 or 3) and next-nearest neighbors (a, b, or c):

$$\tilde{\psi}_1 = \sum_{j=1}^{\infty} \tilde{\psi}_0 \frac{1}{3^j} \tilde{\psi}_0^{2j} [\tfrac{1}{3}\tilde{\psi}_0 + \tfrac{1}{3}\tilde{\psi}_0\tilde{\psi}_1] \tag{3.7}$$

[a similar relation involving $\tilde{\psi}_1$ on both sides can be constructed for the dead-end vertex—it again leads, of course, to the result (3.4)]. The argument s has been omitted in Eq. (3.7) and will henceforth be omitted unless required for clarity. This relation is understood as follows. The first step takes the walker to one of the nearest neighbors 1, 2, or 3, and the Laplace transform of the associated waiting-time distribution for this first

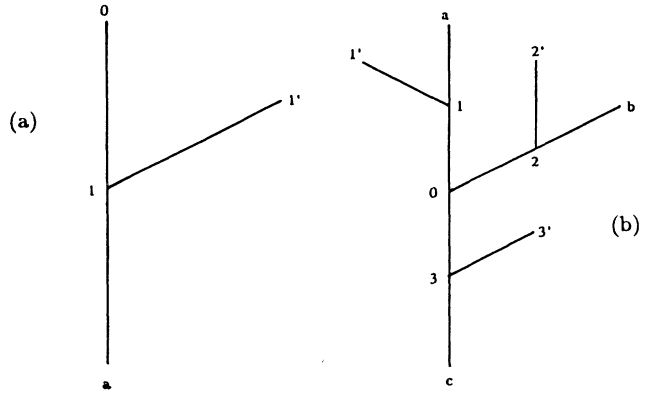

FIG. 2. Decimation procedure for the MV model. (a) The origin 0 is a "dead-end" vertex. Sites 1 and 1′ are removed from explicit consideration by summing over all paths leading through them toward the final destination. Next-nearest-neighbor site a is the final destination of the walk. (b) The origin 0 is a "normal" vertex. The numbered sites are removed from explicit consideration by summing over all the paths through them that lead to either of the three lettered sites.

step is $\tilde{\psi}_0$ [first term on the right-hand side of Eq. (3.7)]. Having reached a nearest neighbor, the walker can now take any number of even steps up and down the branch that emerges from that nearest neighbor (i.e., between 1 and 1′, 2 and 2′, or 3 and 3′). The associated waiting time factor is $\tilde{\psi}_0^{2j}$ and the associated probability per pair of steps is 1/3 (as in the dead-end vertex discussion). This accounts for the second and third terms on the right-hand side of (3.7). Then the walker can either go to the next-nearest neighbor that ends the walk (probability 1/3 and waiting time factor $\tilde{\psi}_0$), as embodied in the first term in square brackets, or it can return to the original vertex 0, from where the walk begins again, as embodied in the second term in square brackets. The sum over j in Eq. (3.7) can be carried out as before, and upon solving for $\tilde{\psi}_1$ we again obtain the relation between $\tilde{\psi}_1$ and $\tilde{\psi}_0$ given in Eq. (3.4). Generalization to further generations then again yields (3.5) and the MV model again gives (3.6). Thus the renormalization equation is independent of the nature of the starting site of the walk. Note also that the known renormalization equations for embedding Euclidean dimensions 1 (see Refs. [9,10]) and 2 are recovered from Eq. (3.6).

All the properties of a random walk on the MV structure can be deduced from the solution $\tilde{\psi}_n(s)$ of the renormalization flow (3.6). Of particular interest is the solution for large n since this yields information about the properties of a random walk at long times and over long distances. Although for the particular case (3.6) it is possible to find an analytic form for the solution at least for small s (which is all that is needed for the analysis of the long-time behavior) [10], for the more complicated renormalization equations that we encounter below this becomes more difficult. We shall be less ambitious and instead concentrate on using the renormalization equation to find $\Psi_n \equiv \tilde{\psi}_n(s=0)$ and $\frac{d\tilde{\psi}_n(s)}{ds}|_{s=0}$. The former is the probability that a hop from the origin to any nth neighbor takes place at all at any time,

$$\Psi_n \equiv \int_0^\infty dt \psi_n(t) = \tilde{\psi}_n(s=0), \tag{3.8}$$

while the latter is the mean time for the walker to first reach any one of the nth neighbors of the origin (also called the mean waiting time or the mean first-passage time),

$$\langle t_n \rangle = \int_0^\infty t\psi_n(t)dt = \left.\frac{d\tilde{\psi}_n(s)}{ds}\right|_{s=0}. \tag{3.9}$$

Thus we first note that the fixed point of Eqs. (3.5) and (3.6) at $s=0$ (i.e., the value of Ψ_n for all n) is unity, that is, the hopping probability from vertex zero to one or another of an arbitrary equidistant set of neighbors is unity. Note, however, that the hopping probability to a *given* one of m equidistant neighbors is $1/m$.

Next consider the behavior of the mean first-passage time to ever more distant neighbors. From (3.6) one can immediately relate the waiting time after the nth decimation to that following the $(n-1)$st decimation using the chain rule

$$\left.\frac{d\tilde{\psi}_n}{ds}\right|_{s=0} = \left.\frac{\partial\tilde{\psi}_n}{\partial\tilde{\psi}_{n-1}}\right|_{s=0} \left.\frac{d\tilde{\psi}_{n-1}}{ds}\right|_{s=0}, \tag{3.10}$$

that is,

$$\langle t_n \rangle = \left.\frac{\partial\tilde{\psi}_n}{\partial\tilde{\psi}_{n-1}}\right|_{s=0} \langle t_{n-1} \rangle. \tag{3.11}$$

From this equation it is easy to see that the factor by which the first-passage time scales from decimation to decimation is given by the term $\left.\frac{\partial\tilde{\psi}_n}{\partial\tilde{\psi}_{n-1}}\right|_{s=0}$. This scaling factor can be calculated immediately from Eq. (3.6) to obtain

$$\left.\frac{\partial\tilde{\psi}_n}{\partial\tilde{\psi}_{n-1}}\right|_{s=0} = 2(d+1) \tag{3.12}$$

and hence

$$\langle t_n \rangle = 2(d+1)\langle t_{n-1} \rangle, \tag{3.13}$$

that is,

$$\langle t_n \rangle = [2(d+1)]^n t_0, \tag{3.14}$$

where $t_0 \equiv \int_0^\infty t\psi_0(t)dt$ is the mean waiting time for a walker to move to a nearest neighbor on the original structure. Recalling that each decimation doubles the distance, we can use this result to calculate the random-walk fractal dimension d_w [15]. Thus, denoting distances by l and times by t we fix d_w by requiring that $l^{d_w} = Dt$ and that $(2l)^{d_w} = 2(d+1)Dt$, where D is a constant of proportionality. Alternatively, if l_0 denotes the nearest-neighbor distance on the original structure, then one requires that $(2^n l_0)^{d_w} = D[2(d+1)]^n t_0$ with $D = l_0^{d_w}/t_0$. In either case this leads to the result

$$d_w = \frac{\ln(d+1)}{\ln 2} + 1. \tag{3.15}$$

Note that with Eq. (3.2) this result agrees with the general relation $d_f = d_w - 1$ for loopless structures [15]. Further, the spectral dimension d_s can be calculated from the relation (definition) $d_s = \frac{2d_f}{d_w}$:

$$d_s = \frac{2\ln(d+1)}{\ln[2(d+1)]}. \tag{3.16}$$

The spectral dimension takes on values smaller than 2, that is, a particle on an MV structure always performs a compact random walk.

It is useful to note the relation between the random walk fractal dimension obtained here in (3.15) and the values of d_w for other familiar cases. Thus, for a random walk on a Euclidean system of any dimension $d_w = 2$. For a Sierpinski gasket one finds $d_w = \ln 5/\ln 2 = 2.322$, that is, it takes longer to cover a given distance on the latter than on the former [10,16]. For the MV structure embedded in two dimensions we find $d_w = 2.585$, that is, passage across a given distance is (not surprisingly in view of the presence of dead ends) even slower than on a Sierpinski gasket. For the MV structure embedded in three dimensions we have $d_w = 3$, which indicates an even longer traversal time of a given distance.

IV. ISOTROPIC RANDOM WALKS ON QUASIRANDOM STRUCTURES

A. Fractal dimensions

The quasirandom model introduced earlier consists of two generators. In order to calculate the fractal dimension of a quasirandom structure we need to average over the occurrence of these two generators. This can be done using the ideas of scaling of the mass and the length used earlier in the calculation of the fractal dimension for the MV model. Since the masses of the generator segments are still all equal at each generation, we can again implement the arguments surrounding Eq. (3.1) and dispense with subscripts. The decimation process is then simply indicated by the scaling of the length. Denoting the average over the occurrence of the two generators by brackets, the mass relation for the quasirandom model then is

$$\langle m(L)\rangle = \sum_k P_{k-1} \sum_{i=1}^{k} m(L/2). \tag{4.1}$$

Here k can take on two values, one for each of the generators, and P_{k-1} is the probability of occurrence of that generator in the structure. For the generator with two collinear units $k = 2$ and the probability of occurrence of this generator is $P_1 \equiv (1 - v)$; for the generator with $(d + 1)$ branches $k = d + 1$ and the probability of occurrence is $P_d \equiv v$. Note that the choice $v = 1$ recovers the MV model. Thus Eq. (4.1) can be rewritten as

$$\langle m(L)\rangle = m(L/2)\sum_k kP_{k-1} = [(d-1)v + 2]m(L/2). \tag{4.2}$$

An increase of the length by a factor of 2 therefore leads to an average increase of the mass by a factor of $[(d - 1)v + 2]$. The resultant fractal dimension is

$$d_f = \frac{\ln[(d-1)v + 2]}{\ln 2}. \tag{4.3}$$

The same approach can be implemented for the generalized quasirandom model. Equation (4.1) still describes the mass scaling, but now k can take on all values between 2 and $d + 1$ with a probability P_k of having a generator made of $k + 1$ units, with $\sum_{k=1}^{d} p_k = 1$. In place of Eq. (4.2) we now have

$$\langle m(L)\rangle = m(L/2)\sum_{k=1}^{d}(k+1)P_k. \tag{4.4}$$

Thus we obtain for the fractal dimension of the generalized quasirandom model

$$d_f = \frac{\ln\left(\sum_{k=1}^{d}(k+1)P_k\right)}{\ln 2}. \tag{4.5}$$

Note that all the models discussed so far can be recovered from the generalized quasirandom model by appropriate choice of the generator probabilities P_k and of the Euclidean embedding dimension d.

B. Renormalization equations and mean waiting times

Here we again implement the decimation procedure discussed in Sec. III B to calculate the renormalization equations for waiting time distributions. For this purpose, we note that there appear three different types of vertices in the quasirandom model, which have been drawn in Fig. 3 for an embedding dimension $d = 2$. Contrary to the MV model where the relation between waiting-time distributions for subsequent generations turned out to be independent of the starting vertex, the distributions for the three vertices here are no longer equal nor are they simply related to one another. We expand our notation to incorporate these different distributions. Thus we denote the waiting-time distribution for a walk originating from a dead-end vertex $\psi^{(1)}(t)$ (the superscript reflects the fact that there is only one way to leave such a vertex). Waiting-time distributions associated with vertices consisting of i units with $i = 2, 3, ..., d + 1$ are similarly denoted by $\psi^{(i)}(t)$.

Consider first the renormalization equations for a walk that originates at a dead-end vertex. There are two contributions to $\psi_n^{(1)}(t)$ as indicated in Fig. 3(a): one arises from the substitution of a unit by the two-collinear-unit generator and the other from substitution by the $(d+1)$-unit generator. The former occurs with probabil-

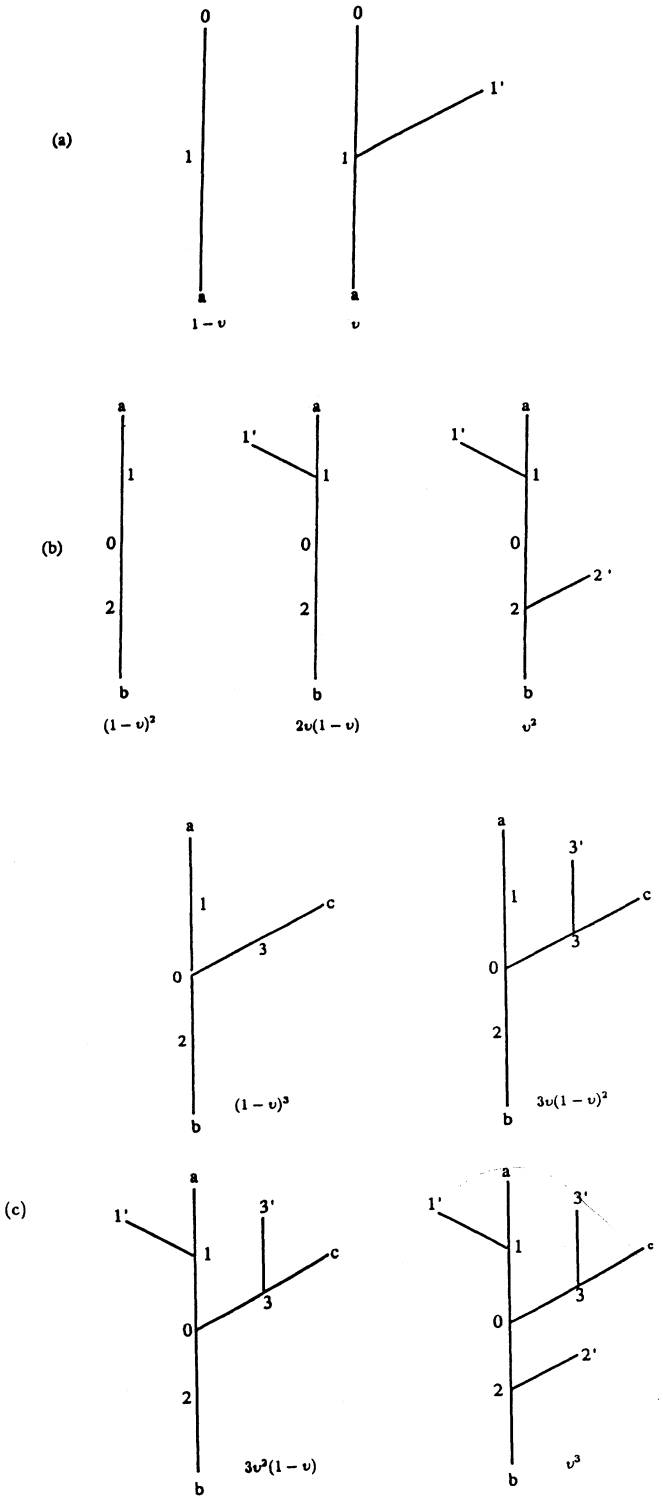

FIG. 3. Decimation procedure for the quasirandom MV model in embedding dimension $d = 2$. (a) The two properly weighted possible configurations with a dead-end vertex as the origin. The walk ends at site a. (b) Three possible configurations if the origin has two emerging branches. The walk ends at either a or b. (c) Four possible configurations if the origin has three emerging branches. The walk ends at a, b, or c.

ity $1-v$, the latter with probability v. The calculation of the renormalization relation is detailed in the Appendix, where we obtain the relation [see Eq. (A5)]

$$\tilde{\psi}_n^{(1)} = (1-v)\frac{\tilde{\psi}_{n-1}^{(1)}\tilde{\psi}_{n-1}^{(2)}}{2-\tilde{\psi}_{n-1}^{(1)}\tilde{\psi}_{n-1}^{(2)}} + v\frac{\tilde{\psi}_{n-1}^{(1)}\tilde{\psi}_{n-1}^{(3)}}{3-2\tilde{\psi}_{n-1}^{(1)}\tilde{\psi}_{n-1}^{(3)}}. \quad (4.6)$$

Next consider a walker who leaves a vertex 0 from which two units emerge. The walker encounters one of the three situations shown in Fig. 3(b). With obvious notation we thus have

$$\tilde{\psi}_n^{(2)} = (1-v)^2\tilde{\psi}_{n,(1-v)^2}^{(2)} + 2v(1-v)\tilde{\psi}_{n,v(1-v)}^{(2)} + v^2\tilde{\psi}_{n,v^2}^{(2)}. \quad (4.7)$$

The factor 2 in the $v(1-v)$ contribution reflects the fact that the side branch can emerge from nearest neighbor 1 or from 2. The three contributions to (4.7) are calculated in the Appendix and are given in Eqs. (A8), (A10), and (A12).

Finally, consider a vertex 0 from which three units emerge. Now the walker encounters one of the four situations shown in Fig. 3(c):

$$\tilde{\psi}_n^{(3)} = (1-v)^3\tilde{\psi}_{n,(1-v)^3}^{(3)} + 3v(1-v)^2\tilde{\psi}_{n,v(1-v)^2}^{(3)} + 3v^2(1-v)\tilde{\psi}_{n,v^2(1-v)}^{(3)} + v^3\tilde{\psi}_{n,v^3}^{(3)}. \quad (4.8)$$

These four contributions are also calculated in the Appendix and are given in Eqs. (A15), (A17), (A19), and (A21).

The properties of a random walk on the quasirandom structure can again be deduced from the renormalization equations. We note that, although the properties of a walk now in general depend on the starting site, the fixed points of Eqs. (4.6), and (4.7) with Eqs. (A8), (A10), and (A12) and of Eq. (4.8) with Eqs. (A15), (A17), (A19), and (A21) are all unity. Thus the hopping probability $\Psi_n^{(i)}$ from any initial site to any one of a set of m equidistant neighbors is again unity, and the probability to a particular neighbor of this set is $1/m$.

The mean first-passage time to reach an nth neighbor of a vertex

$$\langle t_n^{(i)}\rangle = \left.\frac{d\tilde{\psi}_n^{(i)}(s)}{ds}\right|_{s=0}, \quad i = 1,2,\ldots,d+1 \quad (4.9)$$

in general depends on the type of vertex from which the walk starts (i.e., it depends on i), and the renormalization equations yield a set of $(d+1)$ equations connecting the times after the nth decimation to those of the $(n-1)$st decimation:

$$\begin{pmatrix} \langle t_n^{(1)}\rangle \\ \langle t_n^{(2)}\rangle \\ \vdots \\ \langle t_n^{(d+1)}\rangle \end{pmatrix} = \mathbf{J}(0) \begin{pmatrix} \langle t_{n-1}^{(1)}\rangle \\ \langle t_{n-1}^{(2)}\rangle \\ \vdots \\ \langle t_{n-1}^{(d+1)}\rangle \end{pmatrix}. \quad (4.10)$$

The $(d+1)\times(d+1)$ Jacobian matrix $\mathbf{J}(0)$ has elements

$$J_{ij}(0) = \left. \frac{\partial \tilde{\psi}_n^{(i)}(s)}{\partial \tilde{\psi}_{n-1}^{(j)}(s)} \right|_{s=0} \tag{4.11}$$

that can be constructed directly from the renormalization equations [cf. Eqs. (3.11)–(3.14)]. Thus, for example, for $d = 2$ our renormalization equations yield

$$\mathbf{J}(0) = \begin{pmatrix} 2+v & 2(1-v) & 3v \\ v & 2(2-v) & 3v \\ v & 2(1-v) & 2+3v \end{pmatrix}. \tag{4.12}$$

To find the dominant scaling behavior one notes that the solution of (4.10) in analogy with (3.14) is of the form

$$\langle t_n^{(i)} \rangle = (A_1^{(i)} \lambda_1^n + A_2^{(i)} \lambda_2^n + \cdots + A_{d+1}^{(i)} \lambda_{d+1}^n) t_0, \tag{4.13}$$

where t_0 is again the mean hopping time on the original structure. Here the λ_j are the eigenvalues of $\mathbf{J}(0)$ and the n-independent coefficients $A_j^{(i)}$ can easily be obtained in the usual way via the diagonalization of $\mathbf{J}(0)$. For large n, the dominant growth of the $\langle t_n^{(i)} \rangle$ is associated with the largest eigenvalue, say λ_1, which thus determines the scaling of all the $\langle t_n^{(i)} \rangle$ independently of the vertex of origin:

$$\langle t_n^{(i)} \rangle \sim \lambda_1^n t_0. \tag{4.14}$$

The random-walk dimension can thus be read directly from this result [cf. Eq. (3.14) and discussion following]

$$d_w = \frac{\ln \lambda_1}{\ln 2}. \tag{4.15}$$

We have calculated the largest eigenvalue of $\mathbf{J}(0)$ for our quasirandom model and find (for arbitrary d) that $\lambda_1 = 2[(d-1)v + 2]$ (for $d = 2$ the other two eigenvalues are degenerate and are given by $\lambda_2 = \lambda_3 = 2$; the first eigenvalue is therefore sufficiently larger than the other two that it clearly dominates the behavior of the mean waiting time essentially immediately). Thus

$$d_w = \frac{\ln[(d-1)v + 2]}{\ln 2} + 1. \tag{4.16}$$

Note that with (4.3) this result again agrees with the general relation $d_f = d_w - 1$ for loopless structures [15].

It is instructive to compare the value of the random-walk fractal dimension obtained here and the value of d_w found for the MV model in Eq. (3.15). When $v = 1$ the two results are, of course, the same since the quasirandom model then reduces to the MV structure—in this case we found earlier that for $d = 2$, for example, $d_w = 2.585$ while for $d = 3$ we had $d_w = 3$. When $v = 0$ the quasirandom model simply becomes a Euclidean structure and the random-walk dimension accordingly reduces to $d_w = 2$. More interesting is any intermediate situation. For example, when $v = 1/2$, indicating a branching structure with equal probabilities of collinear and treelike generators, we find that $d_w = 2.32$ for $d = 2$ and $d_w = 2.58$ for $d = 3$. A walk across a given distance on a quasirandom fractal structure is clearly slower than on a Euclidean structure but faster than on an MV structure embedded in the same Euclidean dimension.

We conclude our discussion of isotropic diffusion by calculating the renormalization equation for the dead-end vertex in the generalized quasirandom model as an illustration of this generalization. This calculation involves a straightforward extension of the previous analysis. A particular unit is substituted by generators made of $k = 2, 3, \ldots, d+1$ units with respective probabilities P_{k-1}:

$$\tilde{\psi}_n^{(1)} = \sum_{k=1}^{d} P_k \tilde{\psi}_{n,P_k}^{(1)}. \tag{4.17}$$

The reasoning that leads to Eqs. (A2) and (A4) can immediately be generalized to this situation (see the Appendix) to yield

$$\tilde{\psi}_n^{(1)} = \sum_{k=1}^{d} P_k \frac{\tilde{\psi}_{n-1}^{(k+1)} \tilde{\psi}_{n-1}^{(1)}}{k + 1 - k \tilde{\psi}_{n-1}^{(k+1)} \tilde{\psi}_{n-1}^{(1)}}. \tag{4.18}$$

Equation (4.18) and the corresponding ones for the other $\tilde{\psi}_n^{(k)}$ are the most general forms of the isotropic analysis. The scaling of the time can again be found from the largest eigenvalue of the Jacobian that connects the $\langle t_n^{(k)} \rangle$ to the $\langle t_{n-1}^{(k)} \rangle$ and leads to a random-walk dimension that again agrees with that obtained from d_f in (4.5) via the loopless structure relation $d_f = d_w - 1$:

$$d_w = \frac{\ln\left(\sum_{k=1}^{d} (k+1) P_k\right)}{\ln 2} + 1. \tag{4.19}$$

Thus, in general and of course not surprisingly the walk becomes more laborious (slower) as the embedding dimension increases and, in a given dimension, if the structure is more profusely branched.

Note that the associated spectral dimension $d_s = 2d_f/d_w$ for the quasirandom structure is smaller than 2 for any choice of the P_k's and of the embedding dimension d and therefore a walker on these structures always performs a compact random walk.

V. CONCLUSIONS

We have calculated the renormalization equations for unbiased random walks on MV structures and have generalized the discussion to random but loopless DLA-like structures. From these renormalization equations we have calculated the mean time that it takes a random walker to first cover a given distance and from this calculation we have in turn extracted an expression for the random-walk dimension d_w which determines the scaling between the time and the displacement. In all cases we verify the relation $d_f = d_w - 1$ valid for loopless structures [15]. We can of course use the renormalization equations to calculate higher moment properties of our walk such as, for instance, variances of the mean first-passage time. We have not done so in this paper, but rather see this as

setting the framework for the calculations carried out in the companion paper [13] for transport in the presence of an external field. With a field the scaling relations become more complex and direction dependent.

We find that in the unbiased case the behavior of the distance-time scaling is entirely determined by the weighted "branch average"

$$\mathcal{P} \equiv \sum_{k=1}^{d} (k+1) P_k, \tag{5.1}$$

where P_k is the probability of occurrence of a generator with $k+1$ branches. This average is a measure of the proliferation of branches in the structure. After a long time has gone by and the walker has sampled all the possible branching structures it does not matter precisely how these branches are arranged—indeed they could be arranged randomly or different parts of the structure could each contain only one kind of branch. Independently of the site of origin of the walk, we find that the random walk dimension is given by

$$d_w = \frac{\ln \mathcal{P}}{\ln 2} + 1. \tag{5.2}$$

Higher moments of the hopping time distribution in general depend on more detailed features of the branching structure. Furthermore, in the presence of an external field even the mean first-passage time depends on more detailed features of the structure including the angle of the branches relative to the backbone. This dependence is developed further in the following paper [13]. Indeed, Mandelbrot and Vicsek [12] also proposed a model in which, whenever the angle between branches is smaller than $\frac{1}{4}\pi$, randomness is included in the branching orientation. That model is also covered by our isotropic analysis, but the effects of such angle randomness would become apparent in the presence of a field. Our isotropic analysis also holds for any branching structure that has a common site from where all the branches emerge. For all these models Eq. (5.2) is valid.

The similarities in behavior reflected in these results for models that are structurally quite different is in some ways quite encouraging toward our goal of achieving a better understanding of transport phenomena in the real DLA structure. We could further generalize our quasirandom model to admit of generators consisting of $2, \ldots, 2d$ units (where $2d$ is the maximum number of neighbors in the embedding Euclidean dimension). One can use this generalization to construct a structure that obeys the MV rules of no overlap of branches and of no branches appearing below the horizontal hyperplane. In particular, when $d = 2$ we could construct a model where each branch is replaced at the next generation by a generator consisting of 2, 3, or 4 branches with probabilities P_1, P_2, and P_3, respectively. These probabilities as well as the branching angles would be chosen as suggested by experimental and numerical observations [17] so as to most closely mimic the DLA. In making these choices one must observe some restrictions: there is a constraint on the values of P_3 in order to obey the no overlap rule, and the angle between two branches of the four-unit generator must always be smaller than $\frac{\pi}{4}$ in order to ensure that there be no branches below the horizontal. The fractal dimension for this model is again of the form

$$d_f = \frac{\ln \mathcal{P}}{\ln 2} = \frac{\ln \left(\sum_{k=1}^{2d-1} (k+1) P_k \right)}{\ln 2}. \tag{5.3}$$

The random-walk dimension for the unbiased case again follows from (5.3) via the relation $d_f = d_w - 1$, while the properties of this structure in the biased case can be calculated using the procedure of the following paper [13]. Note again that the fact that the structures considered in this paper are loopless implies that d_f fixes the value of the spectral dimension $d_s = 2d_f/d_w$.

Finally, we stress that the results obtained here for the various loopless structures are at least roughly consistent with those obtained for a DLA structure by direct simulations [18]. We can clearly choose probabilities P_k in Eq. (5.3) that lead to the value of d_f appropriate to DLA. This value (to within a few percent of error) has been found from the numerical simulations to be [3] $d_f = 1.7$ for $d = 2$ and $d_f = 2.4$ for $d = 3$. Independent simulations of the random-walk dimension yield $d_w = 2.56$ for $d = 2$ and $d_w = 3.33$ for $d = 3$. These latter numbers are not too different from $d_f + 1 = 2.72$ for $d = 2$ and $d_f + 1 = 3.4$ for $d = 3$ appropriate to loopless structures. The spectral dimension, again calculated independently for the DLA, is in the range $d_s = 1.2 - 1.35$ for $d = 2$ and $d_s = 1.3 - 1.44$ for $d = 3$ (depending on the way that it is calculated). The relation $d_s = 2d_f/(d_f + 1)$ yields the value 1.26 for $d = 2$ and 1.4 for $d = 3$, both within the calculated ranges.

ACKNOWLEDGMENTS

We gratefully acknowledge support from the U.S. Department of Energy Grant No. DE-FG03-86ER13606 and from Grants No. PB91-0222 and No. PB91-0378 of the Dirección General de Investigación Científica y Técnica (Spain).

APPENDIX: RENORMALIZATION EQUATIONS FOR ISOTROPIC MODELS

In this appendix we derive the renormalization equations for the waiting-time distributions $\psi_n^{(k)}$ for the different models considered in the main text. We begin with the waiting-time distributions $\psi_n^{(1)}$, $\psi_n^{(2)}$, and $\psi_n^{(3)}$ for walks originating on the three different types of vertices that arise in the quasirandom model discussed in Sec. IV. We concentrate on the case $d = 2$ shown in Fig. 3.

Consider first a walk that originates at a dead-end vertex. The two possible configurations that arise respectively with probabilities v and $1 - v$ are shown in Fig. 3(a). Instead of first subscripting the waiting-time distributions with 0 for the original lattice and 1 for the once decimated lattice and then observing that the same

relations hold for further generations, we use the subscripts $n-1$ and n from the outset. Thus we wish to calculate the waiting-time distribution $\psi_n^{(1)}(t)$ for passage from the dead-end vertex 0 to site a in terms of the waiting-time distributions for walks through site 1 and where appropriate through site $1'$. For the moment we label the two situations that appear in Fig. 3(a) by a further subscript, v and $1-v$, respectively. Thus consider the waiting-time distribution $\psi_{n,1-v}^{(1)}(t)$ for a walker to go from the vertex 0 to the next-nearest neighbor a for the first of the two cases in the figure. We construct and then explain the relation

$$\tilde{\psi}_{n,1-v}^{(1)} = \tilde{\psi}_{n-1}^{(1)}[\tfrac{1}{2}\tilde{\psi}_{n-1}^{(2)} + \tfrac{1}{2}\tilde{\psi}_{n-1}^{(2)}\tilde{\psi}_{n,1-v}^{(1)}], \tag{A1}$$

where we have omitted the argument s. To reach a, the walker must first go to site 1 (probability 1 and waiting-time distribution $\psi_{n-1}^{(1)}$). From there it can go directly to a (probability $\frac{1}{2}$ and waiting-time distribution $\psi_{n-1}^{(2)}$) or it can return to the original site (probability $\frac{1}{2}$, waiting-time distribution $\psi_{n-1}^{(2)}$) and then start the walk all over again ($\psi_{n,1-v}^{(1)}$). Solving Eq. (A1) for $\tilde{\psi}_{n,1-v}^{(1)}$ we find

$$\tilde{\psi}_{n,1-v}^{(1)} = \frac{\tilde{\psi}_{n-1}^{(1)}(s)\tilde{\psi}_{n-1}^{(2)}(s)}{2-\tilde{\psi}_{n-1}^{(1)}(s)\tilde{\psi}_{n-1}^{(2)}(s)}. \tag{A2}$$

For the second case shown in Fig. 3(a) we similarly reason the relation

$$\tilde{\psi}_{n,v}^{(1)} = \tilde{\psi}_{n-1}^{(1)}\left(\sum_{j=0}^{\infty}(\tfrac{1}{3}\tilde{\psi}_{n-1}^{(3)}\tilde{\psi}_{n-1}^{(1)})^j\right)[\tfrac{1}{3}\tilde{\psi}_{n-1}^{(3)} + \tfrac{1}{3}\tilde{\psi}_{n-1}^{(3)}\tilde{\psi}_{n,v}^{(1)}]. \tag{A3}$$

The walker leaves the vertex 0 (probability 1, waiting-time distribution $\psi_{n-1}^{(1)}$) and goes to site 1. From there it can walk back and forth to site $1'$ any number of times (probability $\frac{1}{3}$ to go from 1 to $1'$ and probability 1 to return to 1, each leg with waiting-time distribution $\psi_{n-1}^{(1)}$). Then the walker can either go to site a to end the walk (probability $\frac{1}{3}$ and waiting time distribution $\psi_{n-1}^{(1)}$) or it can return to the vertex 0 (probability $\frac{1}{3}$ and waiting-time distribution $\psi_{n-1}^{(1)}$) and start all over again ($\psi_{n,v}^{(1)}$). Performing the sum over n and solving for $\tilde{\psi}_{n,v}^{(1)}$ yields

$$\tilde{\psi}_{n,v}^{(1)} = \frac{\tilde{\psi}_{n-1}^{(1)}\tilde{\psi}_{n-1}^{(3)}}{3-2\tilde{\psi}_{n-1}^{(1)}\tilde{\psi}_{n-1}^{(3)}}. \tag{A4}$$

Finally, we combine the results (A2) and (A4) to obtain for the Laplace transform of the waiting-time distribution to go from a dead-end vertex to its $(n+1)$st neighbor the relation

$$\begin{aligned}\tilde{\psi}_n^{(1)} &= (1-v)\tilde{\psi}_{n,1-v}^{(1)} + v\tilde{\psi}_{n,v}^{(1)} \\ &= (1-v)\frac{\tilde{\psi}_{n-1}^{(1)}\tilde{\psi}_{n-1}^{(2)}}{2-\tilde{\psi}_{n-1}^{(1)}\tilde{\psi}_{n-1}^{(2)}} + v\frac{\tilde{\psi}_{n-1}^{(1)}\tilde{\psi}_{n-1}^{(3)}}{3-2\tilde{\psi}_{n-1}^{(1)}\tilde{\psi}_{n-1}^{(3)}}.\end{aligned} \tag{A5}$$

Next consider a walker that leaves a vertex 0 from which two units emerge. In this case we have [cf. Fig. 3(b)]

$$\tilde{\psi}_n^{(2)} = (1-v)^2\tilde{\psi}_{n,(1-v)^2}^{(2)} + 2v(1-v)\tilde{\psi}_{n,v(1-v)}^{(2)} + v^2\tilde{\psi}_{n,v^2}^{(2)}. \tag{A6}$$

The first contribution to (A6) satisfies

$$\tilde{\psi}_{n,(1-v)^2}^{(2)} = \tilde{\psi}_{n-1}^{(2)}[\tfrac{1}{2}\tilde{\psi}_{n-1}^{(2)} + \tfrac{1}{2}\tilde{\psi}_{n-1}^{(2)}\tilde{\psi}_{n,(1-v)^2}^{(2)}] \tag{A7}$$

since the walker first goes to a nearest neighbor (probability 1 and waiting-time distribution $\psi_{n-1}^{(2)}$) and then either goes to a next-nearest neighbor thus ending the walk (probability $\frac{1}{2}$, waiting-time distribution $\psi_{n-1}^{(2)}$) or returns to the origin (probability $\frac{1}{2}$, waiting-time distribution $\psi_{n-1}^{(2)}$ and begins walking again ($\psi_{n,(1-v)^2}^{(2)}$). Solving (A7) yields

$$\tilde{\psi}_{n,(1-v)^2}^{(2)} = \frac{[\tilde{\psi}_{n-1}^{(2)}]^2}{2-[\tilde{\psi}_{n-1}^{(2)}]^2}. \tag{A8}$$

For the second contribution to (A6) we find

$$\begin{aligned}\tilde{\psi}_{n,v(1-v)}^{(2)} &= \tfrac{1}{2}\tilde{\psi}_{n-1}^{(2)}[\tfrac{1}{2}\tilde{\psi}_{n-1}^{(2)} + \tfrac{1}{2}\tilde{\psi}_{n-1}^{(2)}\tilde{\psi}_{n,v(1-v)}^{(2)}] \\ &\quad + \tfrac{1}{2}\tilde{\psi}_{n-1}^{(2)}\left(\sum_{j=0}^{\infty}(\tfrac{1}{3}\tilde{\psi}_{n-1}^{(3)}\tilde{\psi}_{n-1}^{(1)})^j\right) \\ &\quad \times[\tfrac{1}{3}\tilde{\psi}_{n-1}^{(3)} + \tfrac{1}{3}\tilde{\psi}_{n-1}^{(3)}\tilde{\psi}_{n,v(1-v)}^{(2)}],\end{aligned} \tag{A9}$$

which easily leads to

$$\tilde{\psi}_{n,v(1-v)}^{(2)} = \frac{[\tilde{\psi}_{n-1}^{(2)}]^2[3-\tilde{\psi}_{n-1}^{(3)}\tilde{\psi}_{n-1}^{(1)}] + 2\tilde{\psi}_{n-1}^{(2)}\tilde{\psi}_{n-1}^{(3)}}{\{4-[\tilde{\psi}_{n-1}^{(2)}]^2\}[3-\tilde{\psi}_{n-1}^{(3)}\tilde{\psi}_{n-1}^{(1)}] - 2\tilde{\psi}_{n-1}^{(2)}\tilde{\psi}_{n-1}^{(3)}}. \tag{A10}$$

Reasoning in a similar way for the third contribution leads to the relation

$$\begin{aligned}\tilde{\psi}_{n,v^2}^{(2)} &= \tilde{\psi}_{n-1}^{(2)}\left(\sum_{j=0}^{\infty}(\tfrac{1}{3}\tilde{\psi}_{n-1}^{(3)}\tilde{\psi}_{n-1}^{(1)})^j\right) \\ &\quad \times[\tfrac{1}{3}\tilde{\psi}_{n-1}^{(3)} + \tfrac{1}{3}\tilde{\psi}_{n-1}^{(3)}\tilde{\psi}_{n,v^2}^{(2)}],\end{aligned} \tag{A11}$$

from which we immediately obtain

$$\tilde{\psi}_{n,v^2}^{(2)} = \frac{\tilde{\psi}_{n-1}^{(2)}\tilde{\psi}_{n-1}^{(3)}}{3-\tilde{\psi}_{n-1}^{(3)}\tilde{\psi}_{n-1}^{(1)} - \tilde{\psi}_{n-1}^{(2)}\tilde{\psi}_{n-1}^{(3)}}. \tag{A12}$$

A walker that leaves a vertex 0 from which three units emerge encounters the possibilities shown in Fig. 3(c):

$$\begin{aligned}\tilde{\psi}_n^{(3)} &= (1-v)^3\tilde{\psi}_{n,(1-v)^3}^{(3)} + 3v(1-v)^2\tilde{\psi}_{n,v(1-v)^2}^{(3)} \\ &\quad + 3v^2(1-v)\tilde{\psi}_{n,v^2(1-v)}^{(3)} + v^3\tilde{\psi}_{n,v^3}^{(3)}.\end{aligned} \tag{A13}$$

The first contribution to (A13) satisfies

$$\tilde{\psi}_{n,(1-v)^3}^{(3)} = \tilde{\psi}_{n-1}^{(3)}[\tfrac{1}{2}\tilde{\psi}_{n-1}^{(2)} + \tfrac{1}{2}\tilde{\psi}_{n-1}^{(2)}\tilde{\psi}_{n,(1-v)^3}^{(3)}], \tag{A14}$$

which leads to

$$\tilde{\psi}^{(3)}_{n,(1-v)^3} = \frac{\tilde{\psi}^{(3)}_{n-1}\tilde{\psi}^{(2)}_{n-1}}{2-\tilde{\psi}^{(3)}_{n-1}\tilde{\psi}^{(2)}_{n-1}}. \tag{A15}$$

The second contribution to (A13) satisfies

$$\begin{aligned}\tilde{\psi}^{(3)}_{n,v(1-v)^2} &= \tfrac{2}{3}[\tfrac{1}{2}\tilde{\psi}^{(2)}_{n-1} + \tfrac{1}{2}\tilde{\psi}^{(2)}_{n-1}\tilde{\psi}^{(3)}_{n,v(1-v)^2}] \\ &\quad + \tfrac{1}{3}\tilde{\psi}^{(3)}_{n-1}\left(\sum_{j=0}^{\infty}(\tfrac{1}{3}\tilde{\psi}^{(3)}_{n-1}\tilde{\psi}^{(1)}_{n-1})^j\right) \\ &\quad \times[\tfrac{1}{3}\tilde{\psi}^{(3)}_{n-1} + \tfrac{1}{3}\tilde{\psi}^{(3)}_{n-1}\tilde{\psi}^{(3)}_{n,v(1-v)^2}]\end{aligned} \tag{A16}$$

from which one obtains

$$\tilde{\psi}^{(3)}_{n,v(1-v)^2} = \frac{[\tilde{\psi}^{(3)}_{n-1}]^2 + \tilde{\psi}^{(2)}_{n-1}\tilde{\psi}^{(3)}_{n-1}(3-\tilde{\psi}^{(1)}_{n-1}\tilde{\psi}^{(3)}_{n-1})}{(3-\tilde{\psi}^{(2)}_{n-1}\tilde{\psi}^{(3)}_{n-1})(3-\tilde{\psi}^{(1)}_{n-1}\tilde{\psi}^{(3)}_{n-1}) - [\tilde{\psi}^{(3)}_{n-1}]^2}. \tag{A17}$$

The third term in (A13) satisfies

$$\begin{aligned}\tilde{\psi}^{(3)}_{n,v^2(1-v)} &= \tfrac{1}{3}[\tfrac{1}{2}\tilde{\psi}^{(2)}_{n-1} + \tfrac{1}{2}\tilde{\psi}^{(2)}_{n-1}\tilde{\psi}^{(3)}_{n,v^2(1-v)}] \\ &\quad + \tfrac{2}{3}\tilde{\psi}^{(3)}_{n-1}\left(\sum_{j=0}^{\infty}(\tfrac{1}{3}\tilde{\psi}^{(3)}_{n-1}\tilde{\psi}^{(1)}_{n-1})^j\right) \\ &\quad \times[\tfrac{1}{3}\tilde{\psi}^{(3)}_{n-1} + \tfrac{1}{3}\tilde{\psi}^{(3)}_{n-1}\tilde{\psi}^{(3)}_{n,v^2(1-v)}],\end{aligned} \tag{A18}$$

which yields

$$\begin{aligned}&\tilde{\psi}^{(3)}_{n,v^2(1-v)} \\ &\quad = \frac{4[\tilde{\psi}^{(3)}_{n-1}]^2 + \tilde{\psi}^{(2)}_{n-1}\tilde{\psi}^{(3)}_{n-1}(3-\tilde{\psi}^{(1)}_{n-1}\tilde{\psi}^{(3)}_{n-1})}{(6-\tilde{\psi}^{(2)}_{n-1}\tilde{\psi}^{(3)}_{n-1})(3-\tilde{\psi}^{(1)}_{n-1}\tilde{\psi}^{(3)}_{n-1}) - 4[\tilde{\psi}^{(3)}_{n-1}]^2}.\end{aligned} \tag{A19}$$

For the fourth term in (A13) we have

$$\begin{aligned}\tilde{\psi}^{(3)}_{n,v^3} &= \tilde{\psi}^{(3)}_{n-1}\left(\sum_{j=0}^{\infty}(\tfrac{1}{3}\tilde{\psi}^{(3)}_{n-1}\tilde{\psi}^{(1)}_{n-1})^j\right) \\ &\quad \times[\tfrac{1}{3}\tilde{\psi}^{(3)}_{n-1} + \tfrac{1}{3}\tilde{\psi}^{(3)}_{n-1}\tilde{\psi}^{(3)}_{n,v^3}],\end{aligned} \tag{A20}$$

which results in

$$\tilde{\psi}^{(3)}_{n,v^3} = \frac{[\tilde{\psi}^{(3)}_{n-1}]^2}{3-[\tilde{\psi}^{(3)}_{n-1}]^2 - \tilde{\psi}^{(3)}_{n-1}\tilde{\psi}^{(1)}_{n-1}}. \tag{A21}$$

Finally, consider the renormalization equation for the dead-end vertex in the generalized quasirandom model as an illustration of the way in which the calculations are carried out in this more general case. The walker leaves the dead-end vertex and arrives at an intersection from which emerge $k+1$ units. One of these units leads back to the original vertex, one leads to the next-nearest neighbor where the walk ends, and the remaining $k-1$ units lead to other dead ends from which the walker has to return to the intersection, perhaps repeatedly. Our usual reasoning then leads to the relation

$$\begin{aligned}\tilde{\psi}^{(1)}_{n,P_k} &= \tilde{\psi}^{(1)}_{n-1}\left[\sum_{j=0}^{\infty}\left(\frac{k-1}{k+1}\tilde{\psi}^{(k+1)}_{n-1}\tilde{\psi}^{(1)}_{n-1}\right)^j\right] \\ &\quad \times\left[\frac{1}{i+1}\right][\tilde{\psi}^{(k+1)}_{n-1} + \tilde{\psi}^{(k+1)}_{n-1}\tilde{\psi}^{(1)}_{m,P_k}].\end{aligned} \tag{A22}$$

The solution of this equation immediately leads to (4.18).

* Permanent address: Departamento de Física Aplicada I, Universidad Complutense, 28040 Madrid, Spain.

[1] T. A. Witten and L. M. Sanders, Phys. Rev. Lett. **47**, 1400 (1981).

[2] M. Matsushita, M. Sano, Y. Hayakawa, H. Honjo, and Y. Sawada Phys. Rev. Lett. **53**, 286 (1984); Y. Sawada, A. Dougherty, and J. Gollub, *ibid.* **56**, 1260 (1986); D. Grier E. Ben-Jacob, R. Clarke, and L. Sander, *ibid.* **56**, 1264 (1986).

[3] J. K. Kjems, in *Fractals and Disordered Systems*, edited by A. Bunde and S. Havlin (Springer-Verlag, Berlin, 1991).

[4] G. Radnocz, T. Vicseck, L. M. Sander, and D. Grier, Phys. Rev. A **35**, 4012 (1987).

[5] R. Xiao, J. Alexander, and F. Rosenberg, Phys. Rev. A **38**, 2447 (1988).

[6] J. Lee, A. Coniglio, and H. E. Stanley, Phys. Rev. A **41**, 4589 (1990).

[7] J. P. Bouchaud and A. Georges, Phys. Rep. **195**, 127 (1990).

[8] According to the American Heritage Dictionary, the word decimate "should not be used to describe the destruction of any specified percentage other than 10%." It is nevertheless frequently used this way and we follow this colloquial practice.

[9] J. Machta, Phys. Rev. B **24**, 5260 (1981)

[10] C. Van den Broeck, Phys. Rev. Lett. **62**, 1421 (1989); Phys. Rev. A **40**, 7334 (1989); in *Proceedings of the Irreversible Processes and Self-Organization-4 Conference Rostock, 1989*, edited by W. Ebeling and H. Ulbricht (Teubner-Texte zur Physik, Leipzig, 1991).

[11] J. M. R. Parrondo, H. L. Martinez, R. Kawai, and K. Lindenberg, Phys. Rev. A **42**, 723 (1990).

[12] B. B. Mandelbrot and T. Vicsek, J. Phys. A **22**, L377 (1989).

[13] H. L. Martinez, J. M. R. Parrondo, and K. Lindenberg, following paper, Phys. Rev. E **48**, 3556 (1993).

[14] E. W. Montroll and G. H. Weiss, J. Math. Phys. **6**, 167 (1965); E. W. Montroll and B. J. West, *Fluctuation Phenomena*, edited by E. W. Montroll and J. L. Lebowitz (North-Holland, Amsterdam, 1987).

[15] S. Havlin and D. ben-Avraham, Adv. Phys. **36**, 695

(1987).
[16] A. Blumen, J. Klafter, and G. Zumofen, *Optical Spectroscopy of Glasses*, edited by I. Zschokke (Reidel, Dordrecht, 1986).
[17] A. Arneodo, F. Argoul, E. Bacry, J. F. Muzy, and M. Tabard, Phys. Rev. Lett. **68**, 3456 (1992); T. Halsey, P. Meakin, and I. Procaccia, *ibid.* **56**, 854 (1986); P. Meakin, R. C. Ball, R. Ramanlal, and L. M. Sander, Phys. Rev. A **35**, 5233 (1987); P. Ossadnik, *ibid.* **45**, 1058 (1992).
[18] P. Meakin and H. E. Stanely, Phys. Rev. Lett. **51**, 1457 (1983).